Communication—A Simple and Scalable Pre-Lithiation Approach for High Energy and Low Cost Lithium Ion Sulfur Batteries

Journal of The Electrochemical Society, 2020 **167** 060517
1945-7111/2020/167(6)/060517/4/$40.00 © 2020 The Electrochemical Society ("ECS"). Published on behalf of ECS by IOP Publishing Limited

Communication—A Simple and Scalable Pre-Lithiation Approach for High Energy and Low Cost Lithium Ion Sulfur Batteries

Chao Shen,[1,2] Donghao Ye,[1,2,*] Liming Jin,[2,4,5,*] Petru Andrei,[1,2] and Jim P. Zheng[3,,z]**

[1]*Department of Electrical and Computer Engineering, Florida A&M University-Florida State University College of Engineering, Florida 32310, United States of America*
[2]*Aero-Propulsion, Mechatronics and Energy Center, Florida State University, Tallahassee, Florida 32310, United States of America*
[3]*Department of Electrical Engineering, University at Buffalo, The State University of New York, Buffalo, New York 14260, United States of America*
[4]*Clean Energy Automotive Engineering Center, Tongji University, Shanghai 201804, People's Republic of China*
[5]*School of Automotive Studies, Tongji University, Shanghai 201804, People's Republic of China*

Pre-lithiation is an essential technique for development of Li-ion sulfur batteries (LISBs), which have lower cost and higher durability than conventional Li-ion batteries. Herein, a simple and scalable pre-lithiation approach by direct contact with lithium foil is applied to a sulfur-polyacrylonitrile (S-PAN) cathode to construct LISBs, which exhibit an initial capacity of 1367 mAh g^{-1} and maintain 1192 mAh g^{-1} after 100 cycles. Moreover, we demonstrate the feasibility of proposed method on both electrodes for performance enhancement. The theoretical estimation further demonstrates the potential of the system for achieving high specific capacity and good cycle life at low cost.
 [DOI: 10.1149/1945-7111/ab8408]

Manuscript submitted February 9, 2020; revised manuscript received March 5, 2020. Published April 9, 2020.

Supplementary material for this article is available online

Lithium sulfur batteries (LSBs) can provide a theoretical specific energy considerably higher than that of lithium ion batteries (LIBs). Unfortunately, under circumstances such as high sulfur loading, high sulfur content, and low electrolyte/sulfur (E/S) ratio, many of the deficiencies of LSBs are amplified, in particular those associated with lithium anode.[1–4] A possible approach to avoid these issues is to convert LSBs into Li-ion sulfur batteries (LISBs) with a S-based (paired with a pre-lithiated anode) or Li_2S-based (paired with a Li-free anode) cathode.[5] In such configurations, the electrochemical performance of LISBs is decoupled from lithium anode. LISBs are also considered as a safer battery chemistry due to better stability under short-circuit and overcharge/overdischarge conditions.[6,7]

The pre-lithiation is a highly appealing technique to provide additional lithium source and finds its wide application in energy storage devices.[8,9] For LISBs, pre-lithiation is required as the sole lithium source in the system and therefore plays an important role in the overall electrochemical performance. Serval pre-lithiation methods such as ex situ electrochemical method,[5] in situ electrochemical method,[10–12] and chemical lithiation,[13] have been explored in LISBs. Among these works, the utilization of sulfur-polyacrylonitrile (S-PAN) as cathode material deserves considerable attention. S-PAN is a promising cathode material because it has the appealing feature that sulfur is chemically bonded to the polymer backbone, enabling reversible electrochemical reactions without polysulfide dissolution.[14–16] The utilization of S-PAN cathode have been extensively reported,[17–21] among which Shen et al. constructed a high energy LISB using lithium naphthalenide as the pre-lithiation reagent, showing enhanced controllability and efficiency than conventional chemical pre-lithiation.[22]

Here we propose to apply a simple and scalable in situ pre-lithiation approach to a S-PAN cathode and/or graphite anode to construct LISBs. Superior electrochemical performance with a high specific capacity and good cycle life is obtained. We found that the cathode pre-lithiation exhibit even better performance than anode pre-lithiation. Furthermore, we can apply the proposed method to both electrodes simultaneously for performance enhancing. Finally, we conducted a theoretical estimation to further demonstrate the potential of proposed system.

Experimental

Preparation of S-PAN and Li_2S-PAN cathodes and graphite anode.—Sulfur and PAN were mixed (4:1 w:w) and heat treated at 300 °C for 3 h in nitrogen to form a typical S-PAN composite. To prepare the freestanding S-PAN cathode, S-PAN composite and multi-wall carbon nanotubes (MWNTs, 3:1 wt:wt) were dispersed in isopropyl alcohol for ultrasonic dispersion. Here a short (10 μm) and a super-long MWNT (2 mm) are utilized to serve as both conductive network and intercrossed mechanical scaffold. The resulting mixture was vacuum filtered and dried overnight. The composite was directly punched and used as sulfur cathodes with a sulfur loading of 2 mg cm^{-2}.

The Li_2S-PAN cathode was formed in situ by directly contacting the S-PAN cathode with a desired amount of 25-um Li foil (KISCO, Japan) in the presence of LP40 (1 M $LiPF_6$ in ethylene carbonate: diethylene carbonate (1:1 v:v)) electrolyte. The lithiation level corresponds to a specific capacity of ca. 2432 mAh g_s^{-1} based on the applied lithium mass.

For the reference pre-lithiation experiment, a C/S composite cathode [23,24] was contacted directly with the same amount of Li foil in the presence of 1 M LiTFSI and 0.4 M $LiNO_3$ in 1,3-dioxolane/dimethyl ether (1:1 v:v) electrolyte.

The preparation of graphite anode was reported elsewhere.[25] The pre-lithiation of the graphite was conducted in situ by directly contacting the graphite with a desired amount of 25-μm Li foil in the presence of LP40 electrolyte. The lithiation level corresponds to a specific capacity of ca. 351 mAh g^{-1}.

Material characterization.—Crystal structure analysis was carried out by X-ray diffraction (Scintag). The morphologies of the electrodes and element mapping were investigated by scanning electron microscopy (SEM) using a FEI 400 NanoSEM microscope. The sulfur content in the S-PAN composite was determined using chemical analysis (CHNS, Carla Erba 1108).

Electrochemical characterization.—In an argon filled glovebox, CR2032-type coin cells were assembled using Celgard 2400 as the separator and LP40 as the electrolyte. The E/S ratio is ca. 28 ml g^{-1}. The specific capacity and current density were calculated based on

*Electrochemical Society Student Member.
**Electrochemical Society Member.
[z]E-mail: jzheng@buffalo.edu

the weight of sulfur. Cyclic voltammetry (CV) was conducted over a potential range from 1.0 to 3.0 V vs. Li^+/Li at a scan rate of 0.1 mV s^{-1}.

Results and Discussion

As seen in Fig. 1a, the Li_2S-PAN cathode was synthesized by in situ direct contacting the S-PAN cathode with a Li foil in the presence of electrolyte, which have been reported as an efficient approach for lithium ion capacitors.[25,26] The reaction occurs quickly with no signs of polysulfide dissolution in the carbonate electrolyte (see Fig. 1a). By contrast, in the reference experiment where a typical C/S composite cathode was used, a significant amount of polysulfide was generated reflected as an immediate color change in the electrolyte (see Fig. S1 is available online at stacks.iop.org/JES/167/060517/mmedia). Therefore, this method is not suitable for handling conventional sulfur cathodes. However, for S-PAN cathodes, the conversion is very efficient due to the solid-state Li^+ insertion/extraction mechanism, ensuring a one-phase conversion. In addition, the method is scalable for higher loading cathodes, where lithium foils with higher thickness can be used.[25,26]

Figure 1b shows the XRD patterns of the S-PAN and Li_2S-PAN cathode. After pre-lithiation, the obtained peaks matched those of the standard XRD pattern of Li_2S, indicating that the sulfur can be fully lithiated with this simple approach. In S-PAN cathode sulfur appeared in amorphous phase, in agreement with the literature.[14,27–29] The broad diffraction peak at ca. 26° can be indexed as the (002) reflection of the hexagonal graphite structure in MWNT.[30] Figures 1c–1d show the morphologies of the S-PAN and Li_2S-PAN cathodes. The uniform distribution of components was confirmed by element mapping as shown in Fig. S2. Both cathodes share a similar overall morphology, but Li_2S-PAN cathode exhibits an enlarged particle size due to the volume expansion caused by Li^+ incorporation. The sub-micro particles of S-PAN or Li_2S-PAN composites are wrapped with MWNTs, which act as both conductive agent and binder.

The electrochemical performance of the S-PAN and Li_2S-PAN cathodes was then evaluated in Li-S cells. Since an "over-lithiation" is required to account for irreversible reduction of the short (low delocalized) conjugated carbon bonds and the formation of cathode SEI in the initial lithiation of S-PAN,[16,17] we first compared the electrochemical performance of Li_2S-PAN cathodes with different pre-lithiation levels as seen in Table SI. The Li_2S-PAN cathodes with a Li:S weight ratio of the 0.63:1 (corresponding to a lithiation capacity of 2432 mAh g_s^{-1}) shows an optimized performance and was selected for further investigation. Figures 2a–2b present the initial galvanostatic charge-discharge profiles Li-S cells with both cathodes. Note that the cell with Li_2S cathode shows an open-circuit potential of 1.0 V, further confirming the formation of Li_2S. The S-PAN cathode delivers a high discharge capacity of 1458 mAh g^{-1} at second cycle at 0.2 C. Under the same conditions, the Li_2S-PAN cathode shows an even higher capacity of 1593 mAh g^{-1} at second cycle, almost reaching the theoretical capacity. This is possibly because the high potential difference between S-PAN and lithium (ca. 3.0 V) acts as a strong driving force that facilitates the full conversion.[11] The advantage of Li_2S-PAN cathodes can be also observed in the CV curves in Fig. S3. The in situ pre-lithiation process has replaced the first discharge process for S-PAN cathode, which was characterized as a peak at 1.33 V in the first cathodic scan. In addition, the Li_2S-PAN cathode exhibits a better reversibility reflected as a higher overlap of the scan curves.

Figure 2c shows the rate capabilities of the S-PAN and Li_2S-PAN cathodes from 0.1 C to 2 C. Both cathodes demonstrate excellent rate performance while the Li_2S-PAN cathode has higher capacities. Moreover, when the current was changed back to 0.1 C, the cells almost entirely recovered its original reversible capacity, indicating the excellent structural stability and high rate tolerance. The long-term cycling performance is displayed in Fig. 2d. After 100 cycles, Li_2S-PAN still delivers 1441 mAh g^{-1}, above 90% of its initial capacity. The capacity of S-PAN after 100 cycles is 1390 mAh g^{-1}, inferior to the capacity of the Li_2S-PAN cathode. The above results demonstrate that both cathodes can be used successfully for constructing LSBs while Li_2S-PAN cathode has a slightly enhanced electrochemical performance.

Since Li_2S-PAN can function as a Li-rich cathode, it can couple with a Li-free anode to construct LISBs. Herein, graphite was chosen as anode host because of its low cost, high cyclability, and low working potential. Note graphite generally cannot work well in LISBs with ether-based electrolyte due poor SEI formation,[31] while

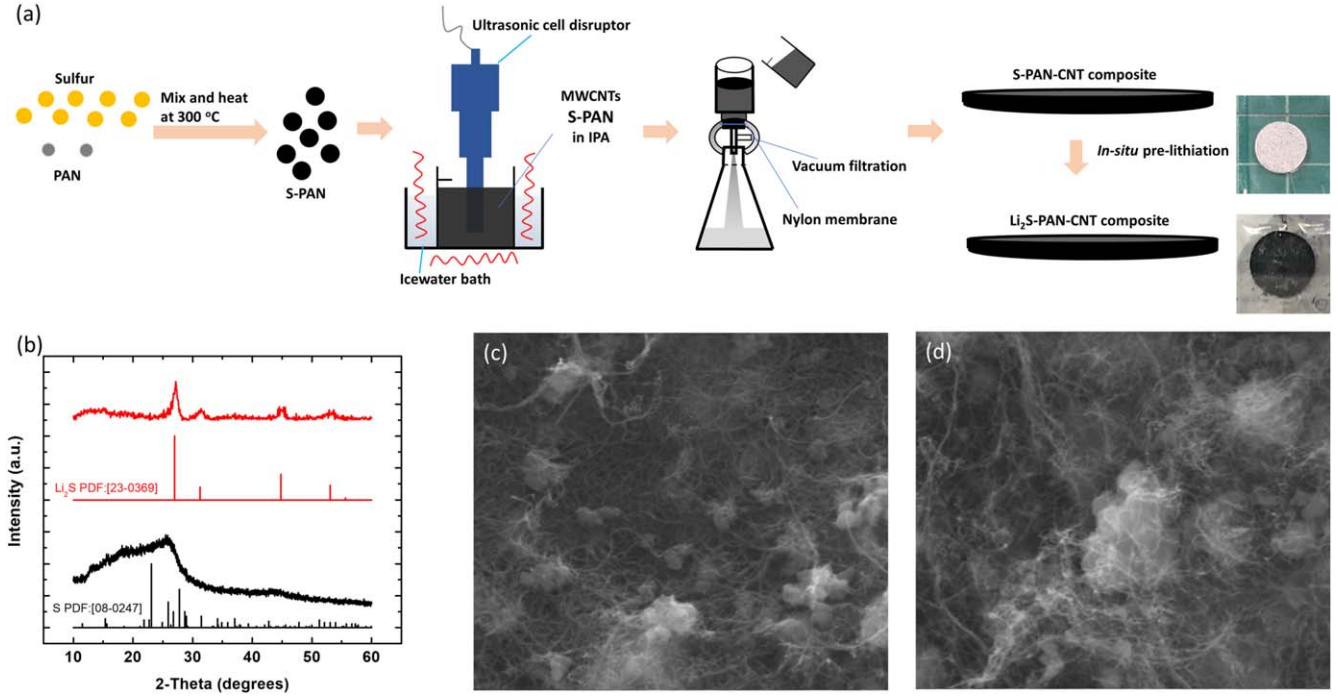

Figure 1. (a) A schematic of synthesis pathway of S-PAN and Li_2S-PAN cathode. (b) XRD pattern of S-PAN and Li_2S-PAN cathode. SEM image of the (c) S-PAN and (d) Li_2S-PAN cathode.

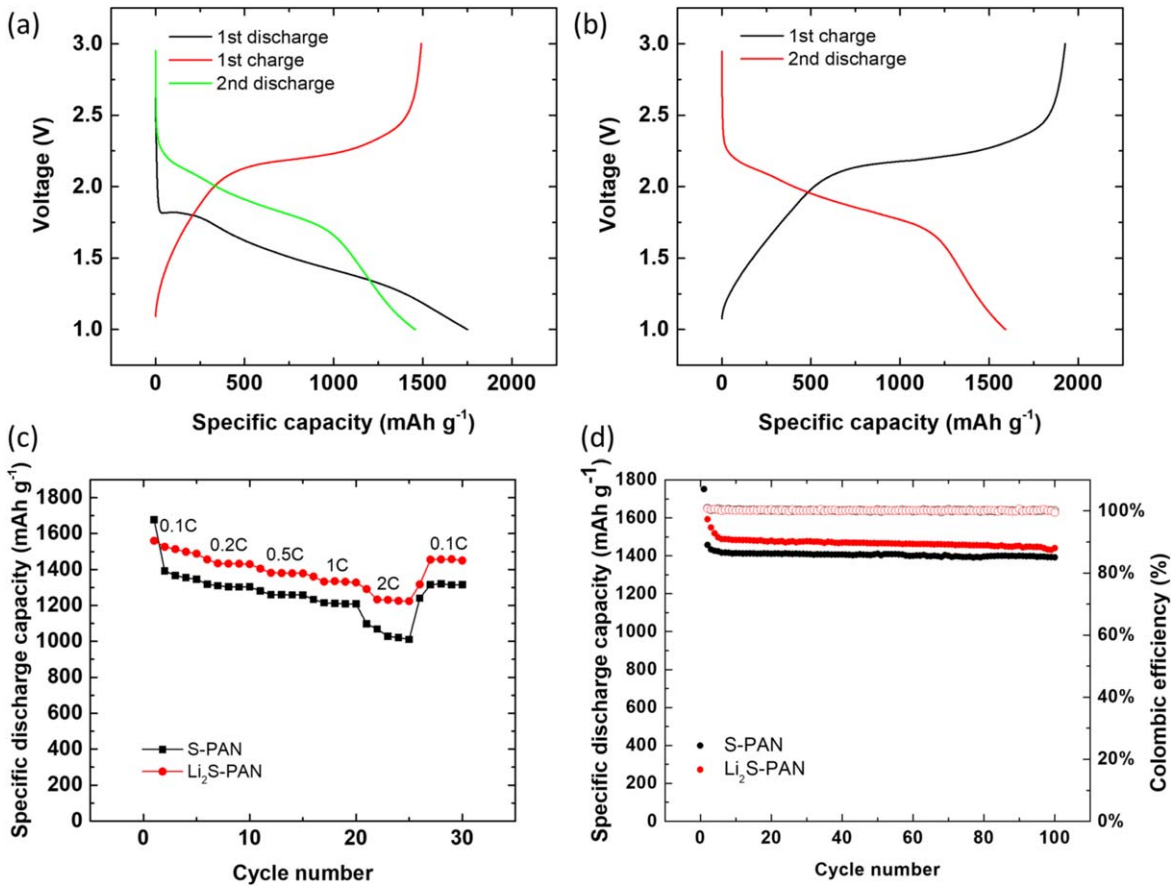

Figure 2. Voltage profiles of Li-S cells with (a) S-PAN and (b) Li_2S-PAN cathodes. (c) Rate capability and (d) cycling performance of Li-S cells at 0.2 C.

this issue is eliminated with the operation of carbonate electrolyte. The full cell voltage profiles are similar to those in Figs. 2a–2b since graphite is operated at near zero voltage. In Fig. 3 we compare their cycling performance. The Li_2S-PAN cell (Li_2S-PAN vs GR) delivers a higher capacity of approximately 1300 mAh g^{-1}. In contrast, the full cell with S-PAN cathode (S-PAN vs GR/Li) has an initial capacity of 1444 mAh g^{-1}, which is significantly reduced to 1213 mAh g^{-1} due to the irreversible reaction during first discharge. As shown in Fig. 3b, Li_2S-PAN vs GR can be cycled over 100 times with a capacity retention of 87%, also superior to S-PAN vs GR/Li.

As we demonstrated in half cell test, the use of Li_2S-PAN cathode yields to a better initial utilization of sulfur. However, for Li_2S-PAN vs GR part of lithium ions from the cathode has to compensate the lithium loss on the anode side during the initial cycles, while for S-PAN vs GR/Li a stable anode SEI is well formed upon cycling. Here, to further compensate this initial anode capacity loss, we applied an additional pre-lithiation process (0.6 wt% of graphite loading, corresponding to 23.2 mAh g^{-1})[25] to the graphite anode to construct Li_2S-PAN vs GR/Li. The obtained cell shows similar first charge capacity with Li_2S-PAN vs GR but highest initial discharge capacity and cycle retention after 100 cycles, indicating that less lithium ions are consumed for anode SEI formation during the initial cycles. In LISBs, both cathode and anode require formation of stable SEI and our proposed pre-lithiation method can be readily applied to both electrodes simultaneously to enable high efficiency of lithium ion utilization.

Finally, the theoretical specific energy and cost of the proposed system based on the experimental results are evaluated in Fig. 4. The details of calculation can be found in the Supplementary Material. In Fig. 4a we plot the specific energy of LISBs with anodes of different effective capacities at different E/S ratios. Since the generation and dissolution of polysulfides are completely eliminated, the electrochemical performance is expected to be less dependent on the E/S

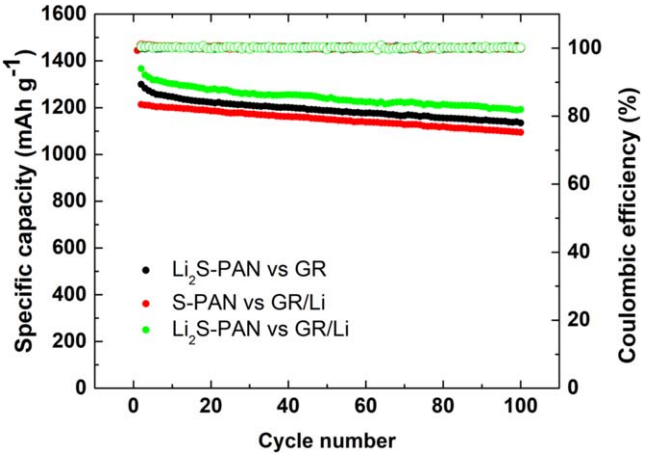

Figure 3. Cycling performance and Coulombic efficiency of the Li-ion sulfur cells at 0.2 C.

ratio than in the case of conventional LSBs.[32–34] This enables the operation of Li/S-PAN battery under a lean electrolyte condition. Despite a relatively low sulfur content in the cathode, at a low E/S ratio, e.g., E/S < 3 ml g^{-1}, the calculated specific energy can be higher than 400 Wh kg^{-1}. In this scenario, the electrolyte volume is mainly determined by the void pore volume of the cathode, and therefore a low porosity cathode with moderate surface area and high tap density is essential to achieve low E/S ratios (see Fig. S4).[35] On the other hand, one can see that when a relatively low capacity anode, e.g., graphite is used, the achievable specific energy of LISBs is limited by the anode capacity rather than the E/S ratio. A hybrid

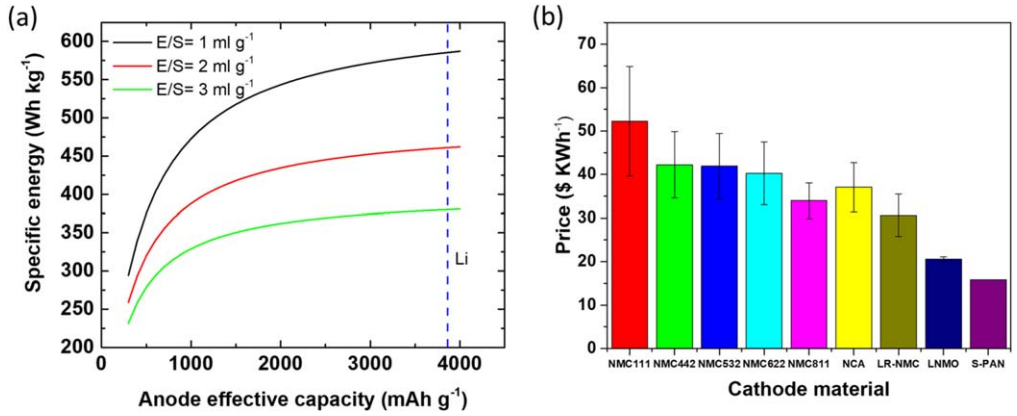

Figure 4. (a) Specific energy of LISB as a function of anode effective capacity. (b) Cost comparison of the S-PAN cathode with other cathode materials in LIBs.

anode such as graphite-silicon composite is preferred to enhance the specific energy of LISBs.[36,37]

Another advantage of LISBs is cost reduction. Figure 4b compares the cost of various cathode materials per KWh, in which the cost of S-PAN based cathode was calculated using the baseline price in Table SII. Note that the cost of lithium for pre-lithiation is also included in calculation and indeed occupy a significant portion of the total cost. One can see that the S-PAN based cathode has the lowest value due to the high capacity of sulfur and low cost of both sulfur and PAN, while the price of other cathode materials heavily depend on the price of the critical constituent metals such as cobalt.[38] On the other hand, the replacement of lithium metal with graphite in LISB also decreases the cost in comparison with LSBs because of the lower excess of Li. Despite a slight increase in the cost due to the introduction of PAN and graphite, the cost of the proposed LISB is comparable with that of conventional LSBs with 140% Li excess, which can be much smaller than the Li excess required for practical operation.[39]

Summary

LISBs exhibit great potential due to the reduced cost and high durability. Regardless of the detailed configuration, the pre-lithiation technique plays a key role for their development. In this work, LISBs based on in situ pre-lithiation of S-PAN cathode and/or graphite anode are constructed, which show excellent electrochemical performance. The effect of different pre-lithiation approaches are evaluated. The theoretical estimation further demonstrates the proposed system as a promising metal-free Li-ion battery with a high specific capacity, good cycle life, and low cost. The development of high-density S-PAN based cathode, optimization and matching with a graphite-silicon composite anode are possible future avenues of study.

Acknowledgments

The work is supported by NSF grant No. 1609860 and 1805288.

ORCID

Jim P. Zheng https://orcid.org/0000-0003-2689-0067

References

1. S. H. Chung, C. H. Chang, and A. Manthiram, *Adv. Funct. Mater.*, **28**, 1801188 (2018).
2. Z.-W. Zhang, H.-J. Peng, M. Zhao, and J.-Q. Huang, *Adv. Funct. Mater.*, **1707536**, 1707536 (2018).
3. M. Rana et al., *Energy Storage Mater.*, 1 (2018).
4. B. Liu, R. Fang, D. Xie, W. Zhang, H. Huang, Y. Xia, X. Wang, X. Xia, and J. Tu, *Energy Environ. Mater.*, **1**, 196 (2018).
5. F. Xu, X. Li, F. Xiao, S. Xu, X. Zhang, P. He, and H. Zhou, *Mater. Technol.*, **31**, 517 (2016).
6. X. Pu, G. Yang, and C. Yu, *Nano Energy*, **9**, 318 (2014).
7. M. Liu, Y. X. X. Ren, H. R. R. Jiang, C. Luo, F. Y. Y. Kang, and T. S. S. Zhao, *Nano Energy*, **40**, 240 (2017).
8. F. Holtstiege, P. Bärmann, R. Nölle, M. Winter, and T. Placke, *Batteries*, **4**, 4 (2018).
9. B. Li et al., *Adv. Mater.*, **1705670**, 1705670 (2018).
10. Y. Wu, T. Yokoshima, H. Nara, T. Momma, and T. Osaka, *J. Power Sources*, **342**, 537 (2017).
11. S. Zheng, Y. Chen, Y. Xu, F. Yi, Y. Zhu, Y. Liu, J. Yang, and C. Wang, *ACS Nano*, **7**, 10995 (2013).
12. M. Weinberger and M. Wohlfahrt-Mehrens, *Electrochim. Acta*, **191**, 124 (2016).
13. Y. Wu, T. Momma, S. Ahn, T. Yokoshima, H. Nara, and T. Osaka, *J. Power Sources*, **366**, 65 (2017).
14. A. Konarov, Z. Bakenov, H. Yashiro, Y. Sun, and S.-T. Myung, *J. Power Sources*, **355**, 140 (2017).
15. W. Wang, Z. Cao, G. A. Elia, Y. Wu, W. Wahyudi, E. Abou-Hamad, A. H. Emwas, L. Cavallo, L. J. Li, and J. Ming, *ACS Energy Lett.*, **3**, 2899 (2018).
16. S. S. Zhang, *Energies*, **7**, 4588 (2014).
17. X. Wang, Y. Qian, L. Wang, H. Yang, H. Li, Y. Zhao, and T. Liu, *Adv. Funct. Mater.*, **1902929**, 1902929 (2019).
18. X. Chen et al., *Nat. Commun.*, **10**, 1021 (2019).
19. S. Li, Z. Han, W. Hu, L. Peng, J. Yang, L. Wang, Y. Zhang, B. Shan, and J. Xie, *Nano Energy*, **60**, 153 (2019).
20. A. N. Arias, A. Y. Tesio, and V. Flexer, *J. Electrochem. Soc.*, **165**, A6119–A6135 (2018).
21. R. Kumar, J. Liu, J. Hwang, and Y. Sun, *J. Mater. Chem. A*, **6**, 11582 (2018).
22. Y. Shen, J. Zhang, Y. Pu, H. Wang, B. Wang, J. Qian, Y. Cao, F. Zhong, X. Ai, and H. Yang, *ACS Energy Lett.*, **4**, 1717 (2019).
23. P. Andrei, C. Shen, and J. P. Zheng, *Electrochim. Acta*, **284**, 469 (2018).
24. C. Shen, J. Xie, M. Zhang, P. Andrei, M. Hendrickson, E. J. Plichta, and J. P. Zheng, *J. Electrochem. Soc.*, **166**, A5287 (2019).
25. A. Shellikeri, V. Watson, D. Adams, E. E. Kalu, J. A. Read, T. R. Jow, J. S. P. S. Zheng, and J. S. P. S. Zheng, *J. Electrochem. Soc.*, **164**, A3914 (2017).
26. W. J. Cao, J. F. Luo, J. Yan, X. J. Chen, W. Brandt, M. Warfield, D. Lewis, S. R. Yturriaga, D. G. Moye, and J. P. Zheng, *J. Electrochem. Soc.*, **164**, A93 (2017).
27. J. Li, K. Li, M. Li, D. Gosselink, Y. Zhang, and P. Chen, *J. Power Sources*, **252**, 107 (2014).
28. A. Konarov, D. Gosselink, T. N. L. Doan, Y. Zhang, Y. Zhao, and P. Chen, *J. Power Sources*, **259**, 183 (2014).
29. P. Chen, Z. Bakenov, A. Konarov, Y. Zhao, and Y. Zhang, *J. Power Sources*, **270**, 326 (2014).
30. C. Shen, J. Xie, T. Liu, M. Zhang, P. Andrei, L. Dong, M. Hendrickson, E. J. Plichta, and J. P. Zheng, *J. Electrochem. Soc.*, **165**, A2833 (2018).
31. L. Wang, Y. Wang, and Y. Xia, *Energy Environ. Sci.*, **8**, 1551 (2015).
32. C. Shen, J. Xie, M. Zhang, P. Andrei, J. P. Zheng, M. Hendrickson, and E. J. Plichta, *J. Power Sources*, **414**, 412 (2019).
33. C. Shen, J. Xie, M. Zhang, J. P. Zheng, M. Hendrickson, and E. J. Plichta, *J. Electrochem. Soc.*, **164**, A1220 (2017).
34. C. Shen, J. Xie, M. Zhang, P. Andrei, M. Hendrickson, E. J. Plichta, and J. P. Zheng, *Electrochim. Acta*, **248**, 90 (2017).
35. A. Bhargav, J. He, A. Gupta, and A. Manthiram, *Joule*, 1 (2020).
36. S. Chae, S.-H. Choi, N. Kim, J. Sung, and J. Cho, *Angew. Chemie*, **59**, 110 201902085 (2019).
37. P. Li, J. Y. Hwang, and Y. K. Sun, *ACS Nano*, **13**, 2624 (2019).
38. M. Wentker, M. Greenwood, and J. Leker, *Energies*, **12**, 1 (2019).
39. J. Chang et al., *Nat. Commun.*, **9**, 1 (2018).